Pseudo-Fovea Formation After Gene Therapy for *RPE65*-LCA

Artur V. Cideciyan,[1] Geoffrey K. Aguirre,[2] Samuel G. Jacobson,[1] Omar H. Butt,[2] Sharon B. Schwartz,[1] Malgorzata Swider,[1] Alejandro J. Roman,[1] Sam Sadigh,[1] and William W. Hauswirth[3]

[1]Scheie Eye Institute, Perelman School of Medicine at the University of Pennsylvania, Philadelphia, Pennsylvania, United States
[2]Department of Neurology, Perelman School of Medicine at the University of Pennsylvania, Philadelphia, Pennsylvania, United States
[3]Department of Ophthalmology, University of Florida, Gainesville, Florida, United States

Correspondence: Artur V. Cideciyan, Scheie Eye Institute, University of Pennsylvania, 51 North 39th Street, Philadelphia, PA 19104, USA; cideciya@mail.med.upenn.edu.

Submitted: October 16, 2014
Accepted: December 12, 2014

Citation: Cideciyan AV, Aguirre GK, Jacobson SG, et al. Pseudo-fovea formation after gene therapy for *RPE65*-LCA. *Invest Ophthalmol Vis Sci*. 2014;56:526–537. DOI:10.1167/iovs.14-15895

Purpose. The purpose of this study was to evaluate fixation location and oculomotor characteristics of 15 patients with Leber congenital amaurosis (LCA) caused by *RPE65* mutations (*RPE65*-LCA) who underwent retinal gene therapy.

Methods. Eye movements were quantified under infrared imaging of the retina while the subject fixated on a stationary target. In a subset of patients, letter recognition under retinal imaging was performed. Cortical responses to visual stimulation were measured using functional magnetic resonance imaging (fMRI) in two patients before and after therapy.

Results. All patients were able to fixate on a 1° diameter visible target in the dark. The preferred retinal locus of fixation was either at the anatomical fovea or at an extrafoveal locus. There were a wide range of oculomotor abnormalities. Natural history showed little change in oculomotor abnormalities if target illuminance was increased to maintain target visibility as the disease progressed. Eleven of 15 study eyes treated with gene therapy showed no differences from baseline fixation locations or instability over an average of follow-up of 3.5 years. Four of 15 eyes developed new pseudo-foveas in the treated retinal regions 9 to 12 months after therapy that persisted for up to 6 years; patients used their pseudo-foveas for letter identification. fMRI studies demonstrated that preservation of light sensitivity was restricted to the cortical projection zone of the pseudo-foveas.

Conclusions. The slow emergence of pseudo-foveas many months after the initial increases in light sensitivity points to a substantial plasticity of the adult visual system and a complex interaction between it and the progression of underlying retinal disease. The visual significance of pseudo-foveas suggests careful consideration of treatment zones for future gene therapy trials. (ClinicalTrials.gov number, NCT00481546.)

Keywords: gene therapy, nystagmus, retinal degeneration

Perception of fine visual detail requires a complex oculomotor system that maintains fixation between a feature of interest and densely packed foveal cone photoreceptors that can signal individually to the visual cortex.[1–4] Many diseases affecting neurons along the retinocortical pathway and their interconnections can result in abnormalities in the oculomotor system, with consequent lack of stable fixation at the fovea. In Leber congenital amaurosis (LCA), for example, abnormalities of the structure and/or function of photoreceptors early during retinal development can interrupt the visual feedback necessary for normal development of the oculomotor system. The result is one of the key pathognomic signs of LCA called sensory defect nystagmus, involuntary and often oscillatory eye movements resulting in instability of fixation.[5] Nystagmus, together with photoreceptor disease and amblyopia, are thought to conspire to reduce visual acuity. Quantitation of the spatiotemporal characteristics of fixation is required not only to interpret the natural history of visual loss in progressive retinal degenerations but also to understand the consequences of modern treatments attempting to modify this natural history.

In 2007, the form of LCA caused by mutations in the *retinal pigment epithelium–specific protein 65kDa* (*RPE65*-LCA) gene became the first hereditary retinal degeneration to be approached with gene augmentation therapy.[6–9] Initial results from independent investigative teams supported the conclusions that the intervention was generally safe and there were improvements in some aspects of visual function but not others. One area of interest without consensus was the effect of gene therapy on nystagmus. One of the groups suggested a "decrease in both monocular and binocular amplitude and frequency of nystagmus" in both treated and untreated eyes, independent of whether the locus of fixation was treated.[7,10] Our group detected no significant differences in nystagmus in any of the eyes treated foveally or extrafoveally or not treated.[9,11] Both studies used a similar range of doses and included some patients with foveal detachments and some without. In addition, in our study there was one patient who slowly developed a pseudo-fovea

by moving her fixation from the anatomical fovea to a treated extrafoveal location,[12] but it was not known whether other patients showed similar results. Other trials have neither confirmed nor contradicted nor expanded upon this observation of pseudo-fovea formation. The current study details the spatiotemporal properties of fixation under retinal imaging performed with carefully controlled ambient light conditions and over a range of targets spanning the visibility threshold of each eye before and after gene therapy in all patients taking part in our clinical trial over a time span that extended up to 6 years.

Methods

Subjects

All procedures complied with the Declaration of Helsinki, and the study was approved by the Institutional Review Board. Informed consent, assent, and parental permission were obtained, and the work was compliant with Health Insurance Portability and Accountability Act. Included were 15 patients taking part in a phase I clinical trial (NCT00481546; www.clinicaltrials.gov) evaluating the safety of rAAV2-CB^{SB}-hRPE65. Individual patient descriptors P1 to P15 used here are identical to those in previous publications of this trial.[8,9,11–14]

Eye Movement and Fixation Monitoring With Retinal Imaging

Eye movements of *RPE65*-LCA patients were recorded by video imaging (25 Hz) of the retina under near-infrared (NIR) illumination, invisible to the subject (MP1; Nidek Technologies America, Inc., Greensboro, NC, USA). All recordings were performed monocularly with the contralateral eye patched. Study and control eyes were tested sequentially. The dark-adapted patients fixated on a continuously illuminated target in a dark room with a black curtain blocking any stray light from reaching the subject's eye. Primary gaze position was used because none of the patients had evidence of a null zone outside the central region when screened with eight targets offset ~15° eccentrically along major and diagonal meridians. The fixation target subtended ~1° in the visual field. Each recording epoch was 30 or 45 seconds; the first 10 seconds was recorded with a reference target known to be visible to the eye, and the remaining time was used to record a test target of lower illuminance. Several epochs were recorded with test targets that straddled the visibility thresholds. Recordings of test targets were sometimes extended to more than 120 seconds to evaluate slow changes in nystagmus waveforms. The reference retinal image obtained at the start of each epoch and the data defining the translation of the reference image during the recording epoch were exported and analyzed.[9,11,12,15,16] The optical coherence tomography-derived location of the foveal depression was used to define the exact location of the anatomical fovea on the reference image. If the mean fixation location was within 1° of the anatomical fovea, fixation was considered "foveal." The frequency of fast eye movements ("jerks") was determined by first calculating the radial distance of the instantaneous retinal fixation locus from the anatomical fovea over time, then filtering the radial extent to obtain the higher frequency component, and finally determining the timing of the local maxima. An overall fixation instability measure based on the upper limit (mean + 2 SD) radial extent was calculated to include both faster and slower eye movement abnormalities as well as time varying amplitudes over each 10-second epoch.

Letter Identification With Retinal Imaging

A series of images of high-contrast, white single letters on a dark background were presented to patients while imaging the retina under NIR illumination (MP1; Nidek Technologies) in order to track fixation location while subjects attempted to recognize each letter presented. Six letters (D, K, C, N, H, and O), which encompass a range of identification difficulties,[17] were available with five heights subtending 0.5° to 3.3° (corresponding to acuity range of ~20/125 to ~20/800). Testing was performed initially with a size that was similar to the clinically determined visual acuity, and the size was increased or decreased based on the identification accuracy obtained. A given size was considered "seen" if identified correctly at least three times in five trials with different letters. Video representations of the letter identification task were generated by applying the horizontal and vertical offset values to a NIR reference image of the fundus (with overlaid features such as the center of anatomical fovea and boundaries of treatment region); each translated image then contributed a single frame of the video, which was played back at the same 25-Hz rate as the original recording.

Functional MRI

A 3-T Trio machine (Siemens Corp., Washington, DC, USA) with an 8-channel Siemens head coil was used to collect echoplanar blood oxygen level-dependent (BOLD) contrast functional magnetic resonance imaging (fMRI) data with whole-brain coverage (repetition time [TR] = 3 seconds; 3- × 3- × 3-mm isotropic voxels; 42 axial slices, interleaved; 64- × 64-voxel in-plane resolution). Nine normally sighted control subjects (20–42 years of age) and two patients (P2 and P10) were studied. Control subjects were studied on one occasion. Patients were studied in two separate sessions held before and after therapy. Head motion was minimized by using foam padding. Participants were dark-adapted prior to scanning. During initial anatomical imaging, dark adaptation was maintained by minimizing stray room light, using opaque shades, covering light sources, and instructing subjects to close their eyes. During functional scanning, the patient was presented with a white rectangular screen of uniform luminance and flickering at 5 Hz for 30-second periods, which then alternated with 30-second periods of darkness. The screen subtended 28° × 18° of visual angle, although light reflected on the bore of the scanner made the effective width of the stimulus considerably larger. This wide-field unstructured stimulus was chosen to obviate the need for fixation in this population of patients with abnormal eye movements and severe vision loss. Stimulus intensity was varied from low to high over a 7.2-log-unit range by sequentially removing neutral density filters from the light path (maximum unattenuated screen luminance = 3.75 log cd · m^{-2}). At least 2 scans of 140 TRs each were performed at each stimulus intensity.

One or more anatomical images were acquired for each subject, using a standard T1-weighted, high-resolution anatomical scan of three-dimensional magnetization prepared rapid gradient echo (3D MPRAGE; 160 slices, 1 × 1 × 1 mm; TR = 1.62 seconds; echo time [TE] = 3.09 ms; inversion time [TI] = 950 ms; field of view [FOV] = 250 mm; flip angle [FA] = 15°). Anatomical data from the subjects were processed using an FMRIB software library version 5.0 toolkit (Analysis Group, FMRIB, Oxford, UK; http://www.fmrib.ox.ac.uk/fsl/) to correct for spatial inhomogeneity and to perform nonlinear noise reduction. Brain surfaces were reconstructed and inflated from the MPRAGE images by using FreeSurfer version 5.1 software (Martinos Center for Biomedical Imaging, Charlestown, MA, USA).[18,19]

Investigative Ophthalmology & Visual Science

Following sinc interpolation in time to correct for the slice acquisition and six parameter least squares motion correction, the echoplanar data were co-registered to subject-specific anatomy in FreeSurfer using FSL-FLIRT with six degrees of freedom under a FreeSurfer wrapper (bbregister). Serial whole-brain (right- and left-hemisphere) surface maps for each individual TR were registered to a common FreeSurfer template surface pseudo-hemisphere (fsaverage_sym) using the FreeSurfer spherical registration system.[20,21] Nuisance covariates included delta transients (periods of raw signal deviation greater than 2 SD from the mean) and head motion as modeled by 3 translation and 3 rotation covariates. The effect of light stimulation was modeled as a step function convolved with a standard hemodynamic response function.[22] The effect of light stimulation, expressed as a percentage change in BOLD signal, was calculated for each subject and for each light level at each vertex within the visual cortex.

A retinotopic atlas for visual (V) areas V1 to V3 based upon cortical surface anatomy was applied to the data.[23,24] Cortical maps of BOLD fMRI effect size were projected onto the visual field out to an eccentricity of 48°. Response maps for V1, V2, and V3 were averaged. This minimized the possibility that points of elevated or decreased signal corresponded to venous anatomy or local cortical folding. The cortical response across stimulus intensity levels was interrogated within the cortical projection site of the treated area of retina, as well as within an isoeccentric control region.

Results

Wide Spectrum of Oculomotor Abnormalities

Partial degeneration of photoreceptors at the fovea combined with abnormally reduced light sensitivity in the remaining photoreceptors[15,25,26] are the major reasons for reduced visual acuity in most patients with *RPE65*-LCA.[15,27–31] When examined cross-sectionally, patients with more abnormal acuity tend to show greater eye movement abnormalities,[15] but fixation and nystagmus characteristics of *RPE65*-LCA have not been studied in detail. We made oculomotor recordings of subjects by using direct retinal imaging monocularly in fully dark-adapted, untreated eyes in a dark room while viewing a stationary target brighter than the visibility threshold of each tested eye.[9,11,12,15] Five *RPE65*-LCA eyes demonstrate the spectrum of oculomotor abnormalities observed under these conditions (Figs. 1A–F). Patient P15 at age 18 with 20/80 acuity and P11 at age 27 with 20/40 acuity showed examples of minor oculomotor abnormalities with foveal fixation. The waveforms had small amplitudes (<1° excursion) and fast movements ("jerks") occurring at 2.0 Hz for P15 and 1.8 Hz for P11 (Figs. 1B, 1C). Fixation instability was 0.8° for both patients, implying that the center of the fixation target fell within 0.8° of the center of the anatomical fovea more than 95% of the time during a typical recording epoch of 10 seconds. Patient P1 at age 24 with 20/250 acuity also showed foveal fixation but with a larger amplitude (~2°) of diagonally beating (1.9-Hz) jerk nystagmus (Fig. 1D); fixation instability was 1.9°. Patient P5, on the other hand, demonstrated a more severe stage of *RPE65*-LCA. At age 20 with 20/2000 acuity, she showed more of a pendular nystagmus waveform (3.3 Hz) with horizontal as well as vertical components of ~4° amplitude and a mean fixation location centered at ~2° superonasal to the fovea; fixation instability around the extrafoveal fixation locus was 2.6° (Fig. 1E). Fifth, P7 at age 15 with 20/250 acuity showed both small and large amplitudes (up to 6°) of nystagmus with jerk and pendular components beating (4 Hz) mostly horizontally across the anatomical fovea (Fig. 1F); fixation instability was 5.1°. In summary, *RPE65*-LCA patients viewing a visible stationary target under controlled adaptation and ambient conditions showed a range of eye movement abnormalities from barely detectable nystagmus with less than 1° amplitude to more severe forms with greater than 6° amplitude beating as fast as 4 Hz frequency.

Influence of Visual Feedback on Nystagmus Characteristics

In patients without a sensory defect, eye movement characteristics are strongly influenced by visual feedback.[32,33] For sensory defect nystagmus in general and for *RPE65*-LCA specifically, the extent of the visual feedback on oculomotor function is unknown. Thus, in a subset of patients, we performed recordings of long duration that included an initial period with a stimulus perceptible to the eye being tested, followed by a longer period without the stimulus. Three examples demonstrate the range of observations in *RPE65*-LCA (Figs. 1G–I). P3 (visual acuity 20/100) showed a horizontally beating nystagmus crossing the fovea with a visible stimulus (Fig. 1G). Upon removal of the visible target, in complete darkness without visible cues there is very little change in the amplitude of the nystagmus as the fixation location slowly drifts nasally away from the fovea, and there is a slight reduction in the frequency of nystagmus (Fig. 1G). P8 (visual acuity 20/160) showed larger amplitude (~3°) horizontal beating jerk nystagmus with a visible target fixating on the fovea (Fig. 1H). Upon removal of the visible target, there was substantial dampening of the nystagmus amplitude and frequency while there was drift of the retina away from where the visible target was earlier (Fig. 1H). P9 (visual acuity 20/100) showed large amplitude (~5°) nystagmus fixating across the fovea when there was a target visible (Fig. 1I). Upon removal of the target, there was initially no change in the amplitude or frequency of the nystagmus for nearly 30 seconds as the fixation location drifted away from the fovea. Afterward however, the jerk component of the nystagmus completely disappeared, and there remained only a slow drift (Fig. 1I).

The effect of *greater* visibility of a target on nystagmus was also evaluated in a subset ($n = 11$) of eyes (Supplementary Fig. S1). Oculomotor recordings were performed in the same session with a standard red reference target (I) chosen to be brighter than the visibility threshold for each patient, as well as with a green target (II) that was photopically matched to the standard target but was ~1 log brighter in scotopic units, and with a red target (III) that was ~0.6 log brighter (in both photopic and scotopic units) than the standard. Representative results from P2 and P6 exhibit similar nystagmus waveforms with greater visibility of targets (Supplementary Fig. S1A). Across all examined subjects, the average instability was 1.63° ± 0.60° with the standard target compared to 1.46 ± 0.82° and 1.43 ± 0.42° with the brighter targets II and III, respectively (Supplementary Fig. S1B). The differences between the brighter and standard targets were not statistically significant (paired *t*-test, $P = 0.51$ for target I vs. II, and $P = 0.25$ for target I vs. III).

These results taken together suggest that in *RPE65*-LCA eyes, interpretation of nystagmus characteristics can be substantially complicated without control and adjustment of the visibility of target to each individual eye at the time of testing. Availability of brighter perceptual cues does not change nystagmus waveform characteristics. However, the loss of visibility of a target, such as may happen with progressive degeneration or as a negative consequence of intervention that causes vision loss, could result in apparent "improvement" of the nystagmus in a subset of patients.

Investigative Ophthalmology & Visual Science

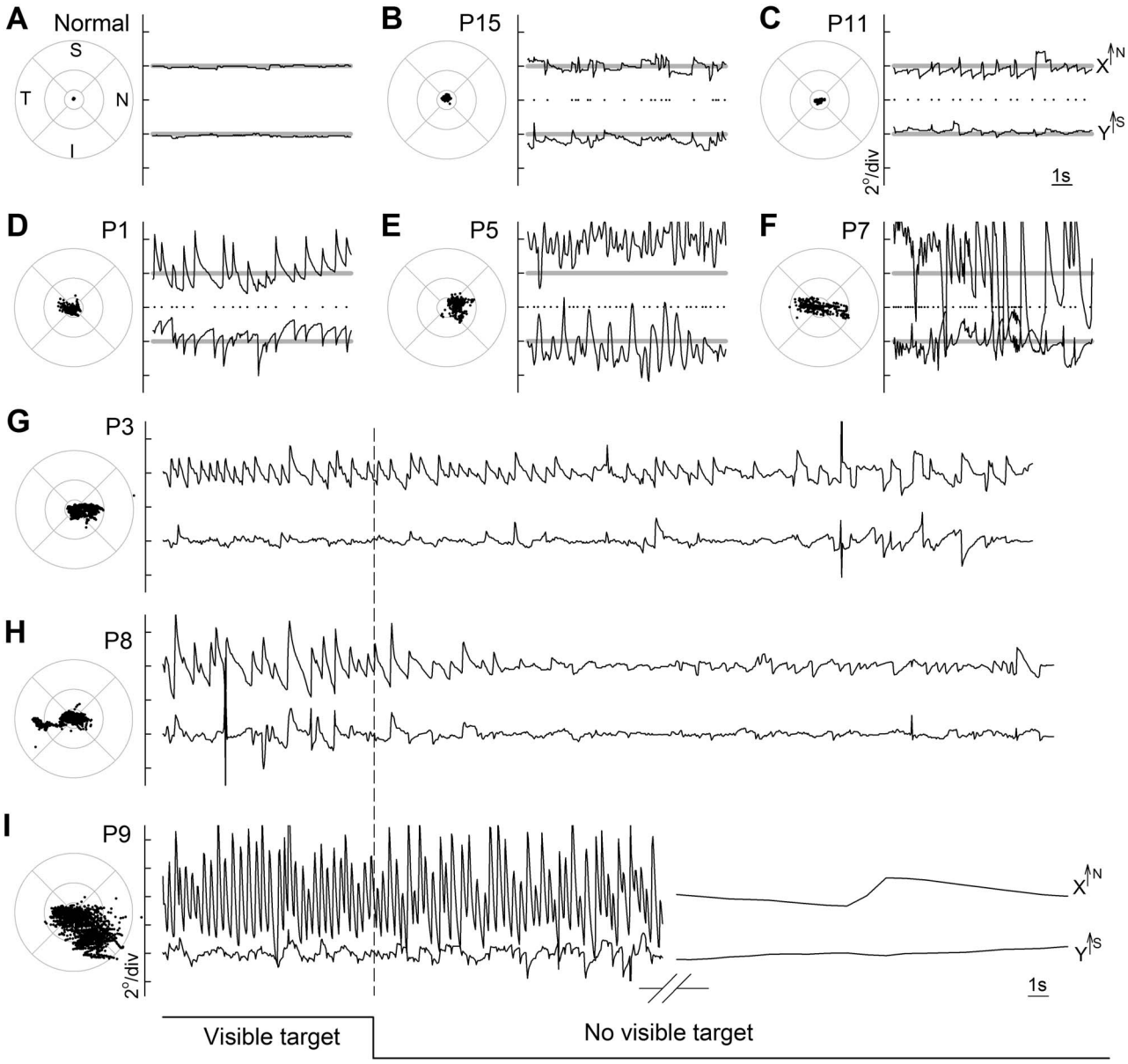

Figure 1. Range of nystagmus features recorded monocularly under direct infrared retinal imaging in dark-adapted patients with *RPE65*-LCA in a dark room viewing a stationary stimulus brighter than the visibility threshold for the eye being recorded. Results from a representative normal subject (**A**) are compared to those of patients (P)15, P11, P1, P5, and P7, respectively (**B–F**). For each subject, 10-second epochs of eye movement data during fixation to a large visible target are shown in spatial and spatiotemporal coordinates. Spatial distribution of fixation clouds are shown on *standard circles* (radii at 1.65°, 5°, and 10°) representing the macular region centered on the anatomical foveal depression. Spatiotemporal distribution of eye movements are shown on chart records for *x* and *y* directions; up is nasal retina for *x* and superior retina for *y*. All results are presented as equivalent right eyes for comparability. *Horizontal gray lines* on the charts show the locations of the anatomical fovea. *Dots* between *x* and *y* traces represent the timing of the high-frequency eye movements used to calculate nystagmus frequency. I, inferior; N, nasal; S, superior; T, temporal retina. (**G–I**) Representative fixation records from P3, P8, and P9 show individual differences in nystagmus waveforms as a function of the visibility of the target in an otherwise darkened ambient environment. Low-frequency components have been removed from the long duration *x-y* chart records (but not from the fixation clouds shown on *standard circles*) in order to better demonstrate nystagmus characteristics as the eyes drift away from the anatomical fovea upon extinction of the visible target. The *break* in axis for P9 represents a period of 25 to 80 seconds.

Natural History of Fixation Location and Stability in *RPE65*-LCA

Serial recordings (over 3.7 ± 1.4 years) in 14 *RPE65*-LCA eyes were used to estimate the natural history of fixation location and stability (Supplementary Table S1). These recordings were performed in the untreated control eyes of patients before and after their gene therapy injections in the contralateral study eyes.[11,14] Twelve of 14 eyes fixated on the fovea (Fig. 2A, half-open symbols) over the follow-up period. Two of 14 eyes (P4 and P5) fixated extrafoveally at baseline and throughout the follow-up period (Fig. 2A, open symbols). Recordings in the control eye of the 15th patient (P10) could not be performed because his severe keratoconus precluded retinal imaging; however, qualitatively (visual judgment of the relative location of the optic nerve), he appeared to fixate extrafoveally.

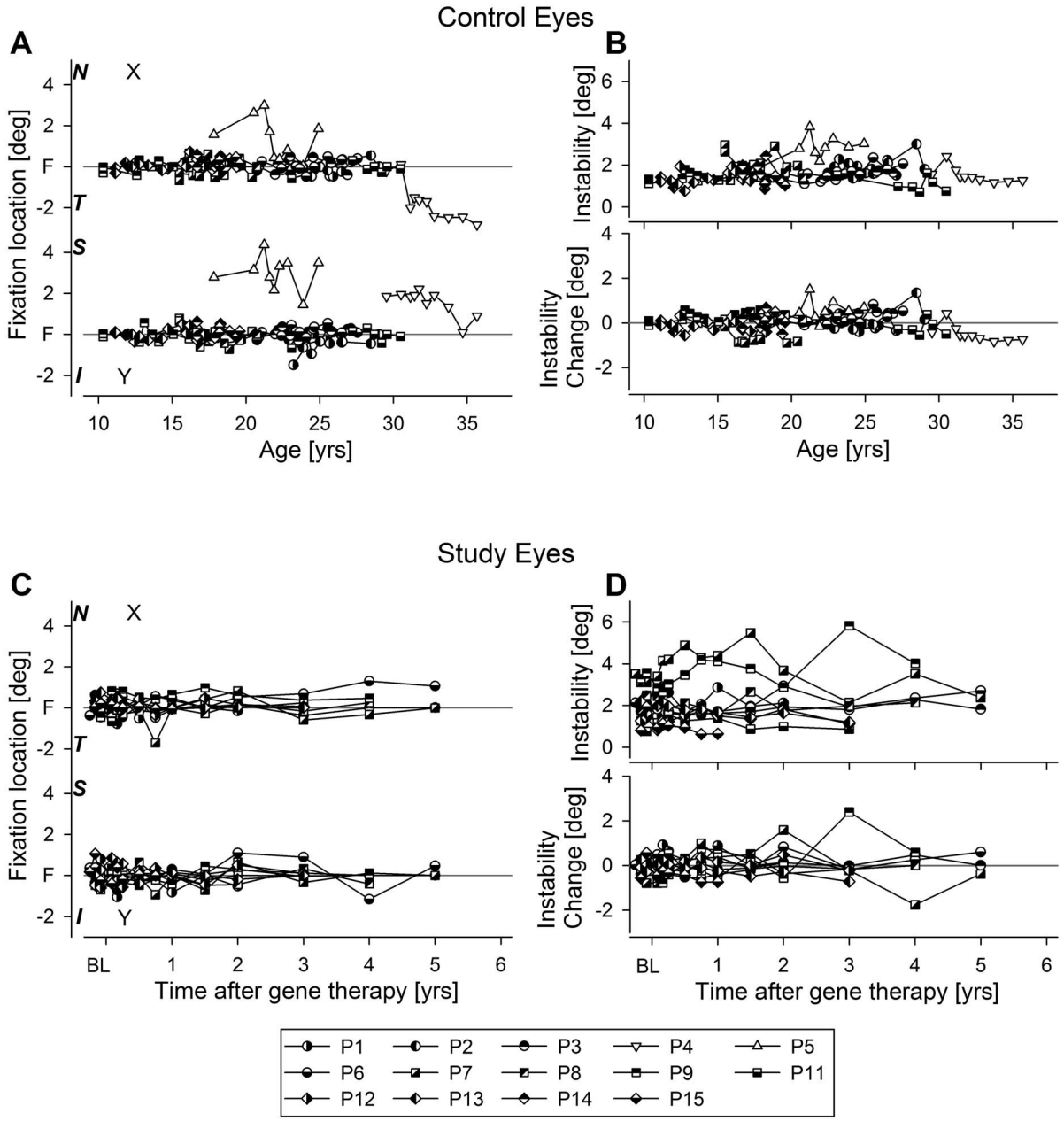

Figure 2. Long-term serial evaluation of fixation location and instability in control (**A**, **B**) and study (**C**, **D**) eyes of *RPE65*-LCA patients. (**A**) Mean fixation location over a 10-second epoch in 14 untreated control eyes (control eye of P10 could not be imaged due to severe keratoconus) along the *horizontal* (*x*) and *vertical* (*y*) axes in terms of the distance from the anatomical fovea. *Open symbols* indicate eyes that retained extrafoveal fixation. (**B**) Fixation instability (*upper*) and its change from the first visit (*lower*) in control eyes. Both fixation location and instability show no significant changes over the duration of serial follow-up. Data are plotted as a function of age at the time of the recording. (**C**) Fixation location in 10 of the 15 study eyes fixating foveally at baseline and post treatment. Baseline (BL) refers to two or three measurements performed before the treatment in the study eye. (**D**) Fixation instability (*upper*) and its change from baseline (*lower*) in 10 of the 15 study eyes. Data are plotted as a function of time after gene therapy.

In 6 of 14 eyes (43%), target illumination needed to be increased during the follow-up period (P1 after 1.5 years, P2 after 6 years, P4 after 6 months, P5 after 9 months, P7 after 18 months, and P8 and P14 after 2 years) in order to retain its visibility. For the remaining eyes, the same target illumination used for baseline recordings remained visible throughout the follow-up period available.

The fixation instability measure ranged from 0.7° to 4° throughout the follow-up period (Fig. 2B, upper panel, half-open symbols). Eyes tended to retain their fixation instability over long-term follow-up without substantial change (Fig. 2B, lower panel). Fixation instability was not related to age ($r^2 = 0.035$; $P = 0.52$).

Fixation Location and Instability After Retinal Gene Therapy

Serial recordings in 15 *RPE65*-LCA study eyes were used to evaluate possible changes to fixation location and instability after retinal gene therapy compared to pretreatment baseline

(Supplementary Table S1). The majority of study eyes (10 of 15) that were foveally fixating at baseline continued to fixate at the fovea postoperatively, independent of whether the treatment detached the fovea (3 of 10 patients) or did not (7 of 10 patients) (Fig. 2C). Two study eyes (P2 and P14) that were fixating foveally at baseline demonstrated pseudo-fovea formation postoperatively and started using two fixation locations depending on the target illuminance (further details below and Fig. 3). Three study eyes (P4, P5, and P10) fixated parafoveally at baseline. Postoperatively, two of them (P4 and P5) showed evidence of an additional pseudo-fovea formation (further details below and Fig. 3), whereas P10 continued to fixate parafoveally after the treatment which detached his fixation locus.

In the 10 eyes without evidence of a new pseudo-fovea formation after gene therapy, instability tended to remain unchanged throughout the follow-up period (Fig. 2D). The fixation instability measure ranged from 0.8° to 4° at baseline and from 0.6° to 6° throughout the follow-up period (Fig. 2D). For 6 of 10 eyes (60%), the same target illumination remained visible throughout the follow-up period; for the remaining four patients (P1 after 1.5 years, P8 after 2 years, P12 after 3 years, and P15 after 1 year), target illumination needed to be increased during the follow-up period in order to retain its visibility.

Emergence and Persistence of Pseudo-Fovea Formation

Four study eyes (P2, P4, P5, P14) showed evidence of either new or additional pseudo-fovea formation post treatment. Previously we described the results in P2, who within the first year after treatment developed a pseudo-fovea.[12] Upon further follow-up, P2 continued to fixate at the (untreated) anatomical fovea with brighter targets for up to 6 years post treatment (Fig. 3A). With dimmer targets that were not perceptible before treatment, she continued to fixate in the (treated) superotemporal retina (Fig. 3A). The mean retinal locus of the pseudo-fovea moved incrementally from ∼12° eccentricity at 1 year, to ∼14° eccentricity at 3 years and to ∼16° eccentricity at 6 years. The outward movement was correlated with localized visual sensitivities showing greater sensitivity at 12° than at 24° eccentric loci at 1 year, whereas by 3 years, the more eccentric locus had slowly gained sensitivity and become more sensitive than the 12° locus. Fixation instability at foveal fixation tended to be much smaller (∼2°) than the instability at the pseudo-fovea locus (7°–9°).

Another patient, P14, had foveal fixation at baseline. Treatment blebs included superior retina and superonasal retina; the fovea was not detached.[11] For 6 months following the treatment, this patient continued to fixate at the fovea. By 9 months, however, she started using a superior retinal pseudo-fovea when detecting a dimmer (previously unseen) target, whereas brighter targets were seen with foveal fixation (Fig. 3B). At her last available visit at year 2, she continued to retain dual pseudo-fovea and fovea fixation depending on the illuminance of the target. Similar to P2, foveal fixation showed smaller instability (∼1.5°) than the instability at the pseudo-fovea (∼4°).

Two additional patients showed examples of new pseudo-fovea formation in a treated region while gradually losing fixation in the region used for fixation at baseline. P4 had an atrophic fovea and fixated on bright targets at a parafoveal region at baseline and for up to 4 years after treatment (Fig. 3C). The treatment bleb included the fovea and the parafoveal and peripapillary regions and extended to the superior retina.[11] Starting ∼1 year post treatment, the patient began to perceive dimmer targets that were not visible before treatment and started using a new pseudo-fovea located near the temporal peripapillary region. Over the next 3 years, the patient retained dual fixation loci that depended upon target luminance; for bright targets, he used the parafoveal fixation he had at baseline and for dimmer targets a peripapillary location that emerged post treatment. By year 5, however, baseline parafoveal fixation was lost, and he started using exclusively the new pseudo-fovea at the peripapillary locus for fixation to a range of perceptible targets (Fig. 3C). There was little difference in instability between the 2 fixation loci (∼2.9° at the parafovea versus ∼2.7° at the peripapillary locus).

Another example of an additional pseudo-fovea emergence was observed in P5. Due to an atrophic fovea, P5 fixated on bright lights parafoveally at baseline and for up to 2 years after the treatment. The treatment included superior and superonasal retina; the foveal region was not detached.[11] Starting ∼1 year post treatment, dimmer lights that were not perceptible before became perceptible when the subject fixated with the superior retina (Fig. 3D). By years 3 and 4, central fixation was lost to both bright and dimmer targets, and all remaining fixation was in the superior retina. Parafoveal fixation showed smaller instability (∼2°) than the superior retinal pseudo-fovea locus (∼6°).

It may be instructive to consider why the remaining 11 of 15 eyes did not show evidence of pseudo-fovea formation as of their last available examination. P10 fixated in the parafoveal region at baseline; the treatment bleb included this region; and after treatment, the patient continued to fixate at the same parafoveal location. P15 has been followed for 1 year; she may still develop a pseudo-fovea in the future. P11 had excellent central vision at baseline, which would be expected to compete with the increased sensitivity in the treated regions. P1 had treatment in the inferior retina, and P3, P7, and P8 had treatments relatively distant from the fovea, thus, likely delaying the emergence of a pseudo-fovea into the future when central vision is lost. P6, P9, P12, and P13 had evidence of amblyopia in the treated eye (there was substantial and historically longstanding interocular asymmetry in visual acuity, even though there was symmetrical foveal outer nuclear layer (ONL) thicknesses) and this may have made it unlikely for a pseudo-fovea to emerge.

Visual Significance of Pseudo-Fovea

To evaluate the real-world significance of the emerging pseudo-foveas in *RPE65*-LCA patients after gene therapy treatment, we performed a letter identification task under direct retinal visualization. P2 at 6 years post treatment was able to consistently identify letters with a height subtending 1.64° (corresponding to ∼20/400 visual acuity) while fixating with the superior-temporal retinal region where a pseudo-fovea had formed 5 years earlier (Supplementary Video S1a). Under these conditions (white letters on a dark background), P2 was able to direct her fixation to the anatomical fovea also and was able to identify the 1.64°-height letters by using the fovea (Supplementary Video S1b). Similar to the fixation task, instability during letter identification with the pseudo-foveal region was greater (∼6.7°) than that using the foveal region (∼2.6°). P2 could not identify the 0.82°-height letters (corresponding to ∼20/200 visual acuity) while fixating with either retinal location.

P4 at 5 years post treatment was able to consistently identify letters with a height subtending 3.3° (corresponding to ∼20/800 visual acuity) while fixating with the peripapillary region where a pseudo-fovea had formed 4 years earlier

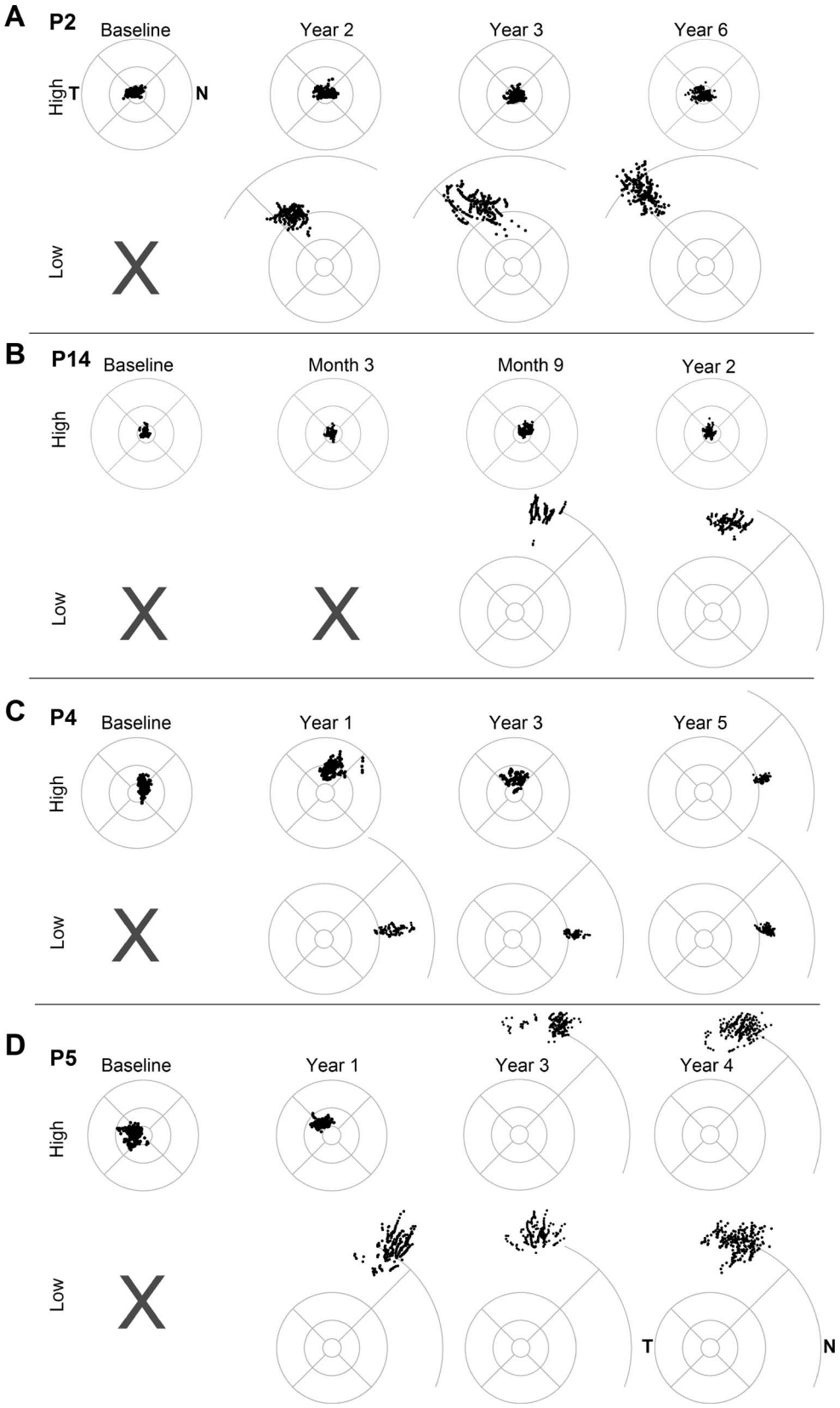

Figure 3. Emergence and persistence of pseudo-fovea in four study eyes of *RPE65*-LCA patients at baseline and at selected times after gene therapy treatment. Fixation clouds are shown for high and low illuminance targets for each patient; *gray x* represents no perception of the low illuminance target. Standard circles represent 1.65°, 5°, and 10° eccentricity from the anatomical fovea; some of the *standard circles* are supplemented with an arc at 20° eccentricity. All eyes are shown as the right eye equivalent for comparability. N, nasal retina; T, temporal retina.

Investigative Ophthalmology & Visual Science

(Supplementary Video S2); at this visit, he never fixated with the anatomical fovea. Fixation instability during the letter recognition task was ~2.5°. P4 could not correctly recognize 1.64°-height letters. When presented with 3.3°-height letters, P5 (3 years post treatment) fixated with the superior retina where a pseudo-fovea had formed and found the location of the letter but could not correctly identify the letters shown. Larger sized letters were not available for testing.

P14 at 9 months post treatment was able to consistently identify letters with a height subtending 3.3° (corresponding to ~20/800 visual acuity) while fixating with the superior retina region where a pseudo-fovea had formed recently (Supplementary Video S3). Fixation instability during the letter recognition task was ~6°. P14 could not correctly recognize 1.64°-height letters with her pseudo-fovea, and she could not locate (or recognize) any letters with her anatomical fovea.

Cortical Correlates of Fixation Location

We examined the cortical response to visual stimulation in two patients. The study eye of P10 had a parafoveal fixation location both prior to and following treatment, which targeted this same region. The study eye of P2 demonstrated emergence of a pseudo-fovea corresponding to the treated retina. We compared the cortical response to visual stimulation before and after treatment in these patients and examined whether the location of fixation corresponded to a relatively preserved area of cortical luminance responsiveness. In normally sighted controls (Fig. 4A), wide-field visual stimulation produced a fairly uniform amplitude of neural response in cortical areas V1 to V3, representing the central 48° of the visual field. These cortical responses may be projected onto the visual field via an anatomical atlas of cortical retinotopic organization that may be applied to both patients and controls.[23,24] The anatomical atlas approach avoids the fundamental limitation that functional retinotopic mapping data are unavailable from within the cortical projection of a scotoma.[34]

In P2 and P10, studied several years prior to therapy (Fig. 4B), responses were restricted to the portion of cortex that represented the macula. When studied 8 years later, the portion of cortex responding to visual stimulation was further contracted. An exception was found within cortical projection of the treated area of retina. There, preserved neural responses to visual stimulation were found. Notably, in P2, the emergence of eccentric fixation was accompanied by loss of cortical sensitivity within the fovea and emergence of a site of responsiveness in an eccentric cortical location.

We examined the amplitude of cortical response as a function of stimulus intensity in the controls and patients (Figs. 4C, 4D). In the normally sighted controls, increasing stimulus luminance was accompanied by an increasing amplitude of neural response averaged over the central 24° representation of visual areas V1 to V3. For the patients, neural response was examined within the cortical projection zone of the treated area of retina, and within a corresponding, isoeccentric control region (Fig. 4D, insets). Within the untreated control region, a decline in neural response across levels of light stimulation was seen between the two measurements made 8 years apart. In contrast, the neural response function was preserved within the treatment projection zone. This effect may be summarized by examining the degree of decline in evoked cortical response between the periods before and after treatment at each light level. Across the three suprathreshold levels of light intensity, the reduction was smaller in the cortical projection of the treated retina (P2 = 0.10% ± 0.19 SEM; P10 = 0.35% ± 0.09 SEM) compared to the untreated retina (P2 = 0.49% ± 0.26 SEM; P10 = 0.60% ± 0.03 SEM).

Discussion

Oculomotor Abnormalities in *RPE65*-LCA

A wide range of oculomotor abnormalities have been reported in patients with retinopathies.[35,36] Onset of retinal disease and the extent of sensory input loss result in different abnormalities. Congenital absence of all vision is often associated with complete lack of gaze control and involuntary roving (or wandering) eye movements.[37] Partial loss of vision occurring congenitally or during early development, on the other hand, can be associated with retained oculomotor control sufficient to allow fixation to a visible target with the remaining vision, but involuntary oscillatory eye movements (often called nystagmus) can cause instability of gaze around the visible target. Instability is thought to result from disrupted maturation of oculomotor circuits that were deprived of critical input during early development.[35] The current study examined LCA patients with *RPE65* mutations across an age range of 10 to 36 years and found that oculomotor abnormalities in this genetically homogeneous cohort spanned a range from barely detectable fixation instability to large amplitude nystagmus beating at a fast frequency. The exact reasons for interindividual differences in nystagmus remain elusive. *RPE65*-LCA eyes with greater ocular instability tend to have lower visual acuity[15] as well as a thinner foveal ONL, but a causative relationship beyond an association remains to be demonstrated. *RPE65*-LCA is a complex disease that involves congenital or very early loss of a portion of photoreceptors and lack of normal visual sensitivity in the remaining photoreceptors. There is also a progressive photoreceptor degeneration.[14,15,38,39] Lack of detectable instability changes in the patients of the current study observed longitudinally over ~4 years and a lack of a relationship between instability and age implicate differences in disease severity at very early ages as the driver for interindividual differences we observed in second and third decades of life.

Contribution of Visual Feedback to Nystagmus

Quantitative properties of nystagmus waveforms can vary for a given individual depending on the environment within which the recordings are being performed. For example, "stress" is thought to increase nystagmus,[40,41] whereas certain nonvisual stimuli have been reported to dampen nystagmus, as least under some conditions.[42,43] What about visual stimuli? Does oculomotor behavior change as a function of the visibility of stimuli on which the patient is asked to fixate? Measurements in blind subjects (including many different clinical diagnoses) performed in darkness have shown that nystagmus waveforms can be present under "open-loop" conditions and do not necessarily require feedback from a visible stimulus to drive the oscillatory eye movements.[37] In the current work, we showed (Fig. 1) that, in complete darkness, some *RPE65*-LCA patients retained their nystagmus characteristics, whereas others showed dampening or complete arrest of nystagmus. These results strongly suggest that reproducible oculomotor recordings in *RPE65*-LCA require strict control of the visual environment.

Fixation at Fovea, Pseudo-Fovea(s), Nystagmus and Consequences of Therapy

Most *RPE65*-LCA patients fixated using their anatomical fovea when presented with a single stationary red stimulus that was brighter than the visibility threshold of each eye. This correlated with retained ONL peaking at the fovea[15,26,38,39] and dark-adapted sensitivity peaking at the fovea[44] in many

Investigative Ophthalmology & Visual Science

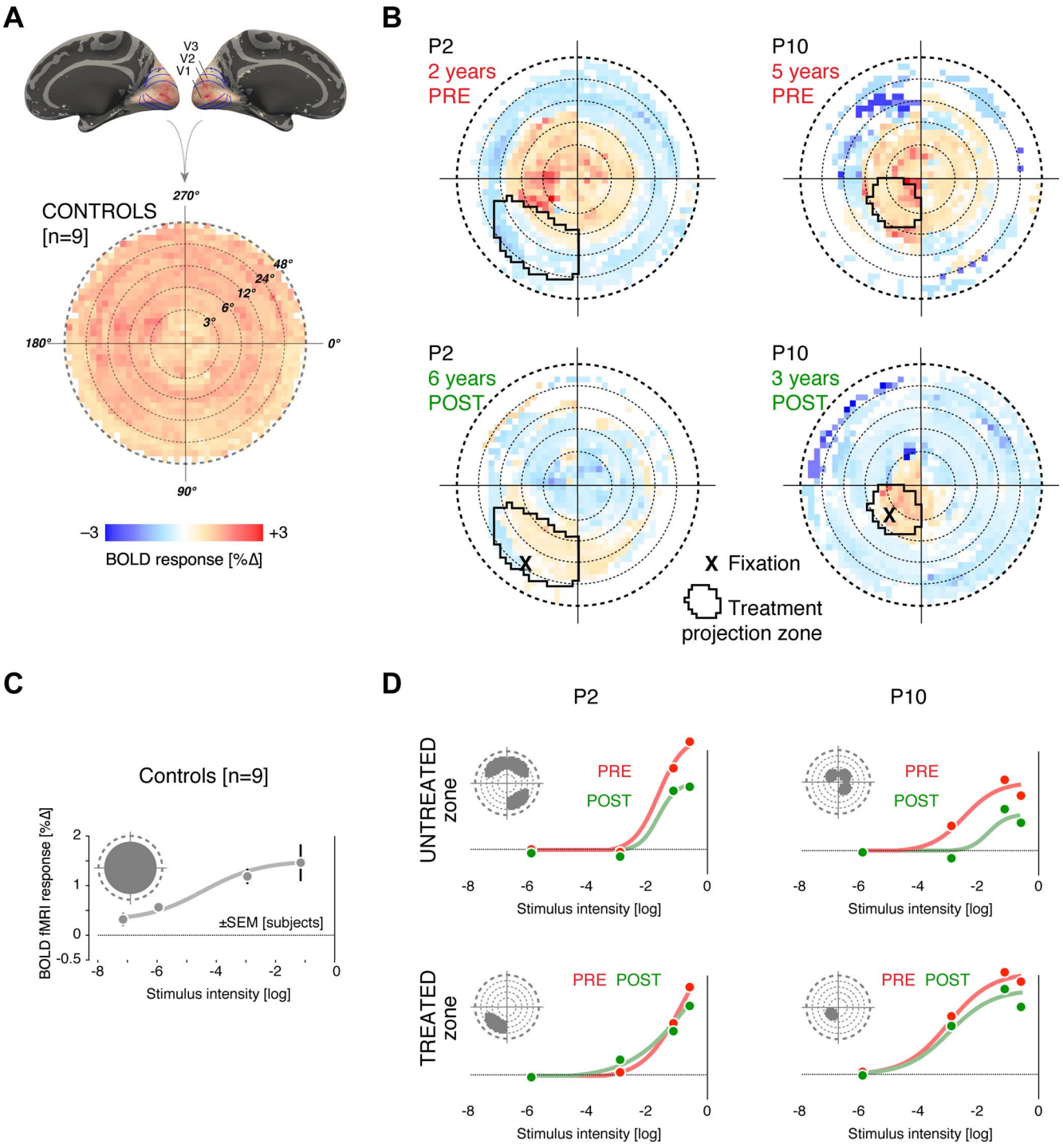

Figure 4. Cortical projection sites of treatment show preserved luminance responses. (**A**, **B**) The visual cortex response to stimulation with a wide-field, flickering stimulus of medium luminance (–3 log) was obtained using BOLD fMRI from patients P2 and P10, several years before and after treatment (**B**) and from nine normally sighted control subjects (**A**). The amplitude of neural response (averaged across V1, V2, and V3) is projected onto the visual field (log eccentricity scale). The *left side* of the plot contains data from the right hemisphere of the brain and thus combines input from the nasal retina of the left eye and temporal retina of the right eye. A uniform amplitude of BOLD response across visual field representation was seen for the control population. For P2 and P10, macular responses are present at 2 and 5 years pretreatment (respectively), but peripheral responses are markedly attenuated. The *black outline* indicates the visual field location of the treated retinal area. In the responses measured at 6 and 3 years post treatment (for P2 and P10, respectively), there has been further loss of macular responses, with the exception of the cortical sites corresponding to the treated area of retina. (**C**, **D**) Each plot provides the amplitude of BOLD fMRI response averaged across V1, V2, and V3, as a function of variation in stimulus luminance. *Inset* in each plot indicates the visual field projection of the cortical region examined. For the control subjects, a steadily increasing cortical response to luminance can be seen (**C**). For P2 and P10, the cortical projection of the isoeccentric, untreated portion of retina ([**D**], *upper row*) was examined pre (*red*) and post treatment (*green*). A marked decrement in response between the two time points is seen. In contrast, within the treatment projection zone ([**D**], *bottom row*) responses at post treatment (*green*) are preserved despite the elapse of nearly 8 years.

Investigative Ophthalmology & Visual Science

RPE65-LCA patients within the first 3 decades of life. After gene therapy, most of the eyes retained fixation at the fovea over the long term. There were, however, four notable exceptions. One exception was noted in follow-up studies performed in a patient we previously described as having a slow emergence of a pseudo-fovea within the treated retinal region.[12] The patient continued to fixate alternately between the fovea and superotemporal pseudo-fovea depending on the visibility of the target. Both fixations were significant for the patient's vision as demonstrated by letter recognition tests. Another patient also demonstrated similarly slow emergence of a pseudo-fovea, which was more useful for letter recognition than her native vision at the fovea. In two patients with foveal atrophy at baseline, a secondary pseudo-fovea emerged in the treated region, whereas their native pseudo-foveas were slowly lost to progressive degeneration. It is important to note that improvements in light sensitivity were detected within days to weeks of treatment, using transient stimuli projected onto retinal locations that would later slowly develop fixation changes to stationary stimuli over a period of a year. These results suggest that cortical adaptations within oculomotor centers may require a relatively long period of new sensory input originating from the treated retinal area.

We found no evidence of decrease in amplitude or frequency of nystagmus in gene therapy-treated eyes, whether treated foveally or extrafoveally; there was also no significant change in fixation stability seen in contralateral untreated eyes. These results are consistent with those of some previously published results[9,11,12] but not of others.[7,10,45,46] This discrepancy may be understood in light of the underlying pathophysiology of the disease and its treatment with gene therapy. Remnant vision in *RPE65*-LCA originates with photoreceptors lacking normal sensitivity to light due to insufficient availability of visual chromophore. Gene augmentation therapy is designed to increase chromophore production within the RPE, and the primary demonstrable result to date is a localized improvement in rod and cone sensitivity.[9,11,13,14] Patients perceive locally increased brightness, sometimes described as a "region of super-vision." However, we showed that substantial increases in brightness of the target (either for rod- or cone-mediated vision) does not significantly alter oculomotor instability (Supplementary Fig. S1). This result is consistent with observation in the clinic, where simply increasing ambient light levels does not dampen the nystagmus. Thus, a potential mechanism linking the reported dampening of the amplitude and frequency of nystagmus[7,10,45,46] to an increase in light sensitivity remains unsupported by available data. Counterintuitively, results compatible to those reported, at least in some patients, may arise from a *loss* of vision (e.g., resulting from a surgically induced macular hole[7] or progressive degeneration) or lack of careful control of the ambient light levels such that visible cues available at baseline were no longer available to patients post treatment.

Acuity Under Retinal Visualization and Fixation Location

Visual acuity in normal eyes (e.g., as measured with the standard Early Treatment Diabetic Retinopathy Study methodology) provides an estimate of the smallest high-contrast letter recognizable by the foveal cone photoreceptors. Loss of visual acuity under retinal degenerative conditions can result from the loss and/or dysfunction of foveal cones, with remaining functional photoreceptors providing the visual acuity measured. These remnant photoreceptors do not have to be foveal (as commonly occurs in maculopathies), nor do they have to be cones (as commonly occurs in achromatopsia). In *RPE65*-LCA, a wide spectrum of visual acuities ranging from nearly 20/20 to light perception (LP) have been reported with typical values in the range of 20/100 to 20/200 for the first 3 decades of life.[15,27–31] Letter recognition tasks under NIR visualization and real-time tracking of the retina, as performed here, allow for better understanding of the use of preferred retinal loci by patients in everyday tasks such as reading. Further development of this technology to a more easily usable form could be valuable as new treatment trials are initiated for retinal degenerative conditions.

Fixation Location and Cortical Function

The distribution of function across the visual field in *RPE65*-LCA is a complex interaction of retinal disease topography, the location and extent of treatment, and the particular stimulus conditions studied. Fixation serves to use the region of the retina with the best visual function for the current circumstances, as reflected in the shifting location of a pseudo-fovea with time and testing conditions.[12] We used fMRI measurement of cortical response to assay function across the visual field in patients over many years of intervening disease progression and therapy to relate the findings to fixation location.

A notable feature of our measurements is that they are linked to retinotopic location. As the rudimentary organization of retinotopic cortex is established prior to visual experience[47] and is tightly linked to cortical surface topology,[23,24] visual cortex function may be related between blind and sighted individuals at precise retinotopic locations, using an anatomical template of retinotopic organization.[48] In *RPE65*-LCA, we find that both the effects of retinal disease and treatment are specific to visual field location. Relatively spared neural responses were found pretreatment in the cortical projection of the macula and within the projection of the treated area of retina years later. Considering the neural response across levels of luminance, we find that the combined effects of 8 years of disease progression plus intervening gene therapy are primarily a preservation of neural response to stimulation at the treated location, as opposed to a response augmentation. This is in contrast to previous fMRI studies performed shortly after therapy in animals and humans[49,50] which reported an increase in cortical response to visual stimulation. Previous human studies in *RPE65*-LCA have measured broad cortical responses across the occipital lobe and used spatial smoothing of the imaging data.[50–52] Although the ability to relate these previous results to a specific retinal locus of treatment is limited, the spatial extent of the observed response in these prior studies nonetheless suggests that it exceeds the cortical projection of the treated area of retina. Further consideration of neural response data within the context of a template of retinotopy and a deeper understanding of the factors that produce local and generalized cortical responses will be crucial to developing fMRI as a measurement of treatment outcome.

We found that the site of preserved cortical response following therapy corresponds to the location of fixation for the two studied patients. In P2, the transition of maximal visual responsiveness from the macula to perifovea was accompanied by a steady shift in the preferred fixation location. The development of a gradually shifting, extrafoveal fixation location is seen as well in age-related macular degeneration (AMD).[53] The cortical response to visual stimulation has also been studied in AMD. Stimulation of either the preferred retinal locus or an isoeccentric location is found to evoke a response in the deafferented portion of visual cortex that represents the fovea.[54,55] Although we did not observe a spread of response to foveal cortex in our patients, this difference between treated *RPE65*-LCA patients and AMD patients is quite understandable. Our stimulus field was wide and unstructured as opposed to

Investigative Ophthalmology & Visual Science

presentation of objects at specific retinal locations. Importantly as well, our patients did not lose all foveal visual function (Supplementary Fig. S2), which has been found to be a critical element for the colonization of foveal cortex by extra-foveal retinal representations.[56,57]

In conclusion, our study quantifies the complexity of eye movements in the *RPE65* form of LCA, not only in the untreated disease but also in eyes treated with gene therapy. Our results suggest that bilateral, localized treatments in *RPE65*-LCA should be placed to allow conjugate pseudo-fovea formation upon loss of central vision to retinal degeneration. Furthermore, a highly practical implication of the results is that interpretation of commonly-used treatment outcomes such as visual acuity needs to be carefully based on knowledge of changes in fixation and formation of pseudo-foveas, either due to treatment effects or foveal atrophy or both.

Acknowledgments

Supported by National Institutes of Health/National Eye Institute Grants EY017280, EY020516, and EY021721. AVC is a Research to Prevent Blindness Senior Scientific Investigator. The sponsor or funding organization had no role in the design or conduct of this research. AVC, SGJ, and WWH are co-inventors on a pending patent application by the University of Pennsylvania and University of Florida on "AAV-mediated gene therapy for *RPGR* X-linked retinal degeneration"; SGJ and WWH are co-inventors on a patent held by the University of Pennsylvania, University of Florida, and Cornell University on "A method for treating or retarding the development of blindness," but SGJ has waived all financial gain; WWH and the University of Florida have a financial interest in the use of AAV therapies and own equity in AGTC, Inc.

Disclosure: **A.V. Cideciyan**, P; **G.K. Aguirre**, None; **S.G. Jacobson**, P; **O.H. Butt**, None; **S.B. Schwartz**, None; **M. Swider**, None; **A.J. Roman**, None; **S. Sadigh**, None; **W.W. Hauswirth**, AGTC (I)

References

1. Putnam NM, Hofer HJ, Doble N, Chen L, Carroll J, Williams DR. The locus of fixation and the foveal cone mosaic. *J Vis*. 2005; 5(7):632–639.
2. Wurtz RH. Neuronal mechanisms of visual stability. *Vision Res*. 2008;48:2070–2089.
3. Rossi EA, Roorda A. The relationship between visual resolution and cone spacing in the human fovea. *Nat Neurosci*. 2010;13: 156–157.
4. Kowler E. Eye movements: the past 25 years. *Vision Res*. 2011; 51:1457–1483.
5. Weiss AH, Biersdorf WR. Visual sensory disorders in congenital nystagmus. *Ophthalmology*. 1989;96:517–523.
6. Bainbridge JW, Smith AJ, Barker SS, et al. Effect of gene therapy on visual function in Leber's congenital amaurosis. *N Engl J Med*. 2008;358:2231–2239.
7. Maguire AM, Simonelli F, Pierce EA, et al. Safety and efficacy of gene transfer for Leber's congenital amaurosis. *N Engl J Med*. 2008;358:2240–2248.
8. Hauswirth WW, Aleman TS, Kaushal S, et al. Treatment of Leber congenital amaurosis due to RPE65 mutations by ocular subretinal injection of adeno-associated virus gene vector: short-term results of a phase I trial. *Hum Gene Ther*. 2008;19: 979–990.
9. Cideciyan AV, Aleman TS, Boye SL, et al. Human gene therapy for RPE65 isomerase deficiency activates the retinoid cycle of vision but with slow rod kinetics. *Proc Natl Acad Sci U S A*. 2008;105:15112–15117.
10. Maguire AM, High KA, Auricchio A, et al. Age-dependent effects of RPE65 gene therapy for Leber's congenital amaurosis: a phase 1 dose-escalation trial. *Lancet*. 2009;374:1597–1605.
11. Jacobson SG, Cideciyan AV, Ratnakaram R, et al. Gene therapy for Leber congenital amaurosis caused by RPE65 mutations: safety and efficacy in 15 children and adults followed up to 3 years. *Arch Ophthalmol*. 2012;130:9–24.
12. Cideciyan AV, Hauswirth WW, Aleman TS, et al. Vision 1 year after gene therapy for Leber's congenital amaurosis. *N Engl J Med*. 2009;361:725–727.
13. Cideciyan AV, Hauswirth WW, Aleman TS, et al. Human RPE65 gene therapy for Leber congenital amaurosis: persistence of early visual improvements and safety at 1 year. *Hum Gene Ther*. 2009;20:999–1004.
14. Cideciyan AV, Jacobson SG, Beltran WA, et al. Human retinal gene therapy for Leber congenital amaurosis shows advancing retinal degeneration despite enduring visual improvement. *Proc Natl Acad Sci U S A*. 2013;110:E517–E525.
15. Jacobson SG, Aleman TS, Cideciyan AV, et al. Human cone photoreceptor dependence on RPE65 isomerase. *Proc Natl Acad Sci U S A*. 2007;104:15123–15128.
16. Cideciyan AV, Swider M, Aleman TS, et al. Macular function in macular degenerations: repeatability of microperimetry as a potential outcome measure for ABCA4-associated retinopathy trials. *Invest Ophthalmol Vis Sci*. 2012;53:841–852.
17. Ferris FL III, Kassoff A, Bresnick GH, Bailey I. New visual acuity charts for clinical research. *Am J Ophthalmol*. 1982;94: 91–96.
18. Dale AM, Fischl B, Sereno MI. Cortical surface-based analysis: I. Segmentation and surface reconstruction. *Neuroimage*. 1999; 9:179–194.
19. Fischl B, Dale AM. Measuring the thickness of the human cerebral cortex from magnetic resonance images. *Proc Natl Acad Sci U S A*. 2000;97:11050–11055.
20. Fischl B, Sereno MI, Tootell RB, Dale AM. High-resolution intersubject averaging and a coordinate system for the cortical surface. *Hum Brain Mapp*. 1999;8:272–284.
21. Greve DN, Van der Haegen L, Cai Q, et al. A surface-based analysis of language lateralization and cortical asymmetry. *J Cogn Neurosci*. 2013;25:1477–1492.
22. Aguirre GK, Zarahn E, D'Esposito M. The variability of human, BOLD hemodynamic responses. *Neuroimage*. 1998;8:360–369.
23. Benson NC, Butt OH, Datta R, Radoeva PD, Brainard DH, Aguirre GK. The retinotopic organization of striate cortex is well predicted by surface topology. *Curr Biol*. 2012;22:2081–2085.
24. Benson NC, Butt OH, Brainard DH, Aguirre GK. Correction of distortion in flattened representations of the cortical surface allows prediction of V1-V3 functional organization from anatomy. *PLoS Comput Biol*. 2014;10:e1003538.
25. Jacobson SG, Cideciyan AV, Aleman TS, et al. RDH12 and RPE65, visual cycle genes causing Leber congenital amaurosis, differ in disease expression. *Invest Ophthalmol Vis Sci*. 2007; 48:332–338.
26. Maeda T, Cideciyan AV, Maeda A, et al. Loss of cone photoreceptors caused by chromophore depletion is partially prevented by the artificial chromophore pro-drug, 9-cis-retinyl acetate. *Hum Mol Genet*. 2009;18:2277–2287.
27. Paunescu K, Wabbels B, Preising MN, Lorenz B. Longitudinal and cross-sectional study of patients with early-onset severe retinal dystrophy associated with RPE65 mutations. *Graefes Arch Clin Exp Ophthalmol*. 2005;243:417–426.
28. Lorenz B, Poliakov E, Schambeck M, Friedburg C, Preising MN, Redmond TM. A comprehensive clinical and biochemical functional study of a novel RPE65 hypomorphic mutation. *Invest Ophthalmol Vis Sci*. 2008;49:5235–5242.

29. Walia S, Fishman GA, Jacobson SG, et al. Visual acuity in patients with Leber's congenital amaurosis and early childhood-onset retinitis pigmentosa. *Ophthalmology*. 2010;117:1190–1198.
30. Weleber RG, Michaelides M, Trzupek KM, Stover NB, Stone EM. The phenotype of severe early childhood onset retinal dystrophy (SECORD) from mutation of RPE65 and differentiation from Leber congenital amaurosis. *Invest Ophthalmol Vis Sci*. 2011;52:292–302.
31. Roman AJ, Cideciyan AV, Schwartz SB, Olivares MB, Heon E, Jacobson SG. Intervisit variability of visual parameters in Leber congenital amaurosis caused by RPE65 mutations. *Invest Ophthalmol Vis Sci*. 2013;54:1378–1383.
32. Abadi RV, Scallan CJ. Waveform characteristics of manifest latent nystagmus. *Invest Ophthalmol Vis Sci*. 2000;41:3805–3817.
33. Wiggins D, Woodhouse JM, Margrain TH, Harris CM, Erichsen JT. Infantile nystagmus adapts to visual demand. *Invest Ophthalmol Vis Sci*. 2007;48:2089–2094.
34. Sunness JS, Liu T, Yantis S. Retinotopic mapping of the visual cortex using functional magnetic resonance imaging in a patient with central scotomas from atrophic macular degeneration. *Ophthalmology*. 2004;111:1595–1598.
35. Leigh RJ, Zee DS. Eye movements of the blind. *Invest Ophthalmol Vis Sci*. 1980;19:328–331.
36. Hall EC, Gordon J, Hainline L, Abramov I, Engber K. Childhood visual experience affects adult voluntary ocular motor control. *Optom Vis Sci*. 2000;77:511–523.
37. Hall EC, Gordon J, Abel LA, Hainline L, Abramov I. Nystagmus waveforms in blindness. *Vis Impair Res*. 2000;2:65–73.
38. Jacobson SG, Aleman TS, Cideciyan AV, et al. Identifying photoreceptors in blind eyes caused by RPE65 mutations: prerequisite for human gene therapy success. *Proc Natl Acad Sci U S A*. 2005;102:6177–6182.
39. Jacobson SG, Cideciyan AV, Aleman TS, et al. Photoreceptor layer topography in children with leber congenital amaurosis caused by RPE65 mutations. *Invest Ophthalmol Vis Sci*. 2008;49:4573–4577.
40. Cham KM, Anderson AJ, Abel LA. Oscillopsia and the influence of stress and motivation in fusion maldevelopment nystagmus syndrome. *Invest Ophthalmol Vis Sci*. 2013;54:2004–2010.
41. Jones PH, Harris CM, Woodhouse JM, Margrain TH, Ennis FA, Erichsen JT. Stress and visual function in infantile nystagmus syndrome. *Invest Ophthalmol Vis Sci*. 2013;54:7943–7951.
42. Nau A, Hertle RW, Yang D. Effect of tongue stimulation on nystagmus eye movements in blind patients. *Brain Struct Funct*. 2012;217:761–765.
43. Beh SC, Tehrani AS, Kheradmand A, Zee DS. Damping of monocular pendular nystagmus with vibration in a patient with multiple sclerosis. *Neurology*. 2014;82:1380–1381.
44. Jacobson SG, Aleman TS, Cideciyan AV, et al. Defining the residual vision in leber congenital amaurosis caused by RPE65 mutations. *Invest Ophthalmol Vis Sci*. 2009;50:2368–2375.
45. Simonelli F, Maguire AM, Testa F, et al. Gene therapy for Leber's congenital amaurosis is safe and effective through 1.5 years after vector administration. *Mol Ther*. 2010;18:643–650.
46. Testa F, Maguire AM, Rossi S, et al. Three-year follow-up after unilateral subretinal delivery of adeno-associated virus in patients with Leber congenital Amaurosis type 2. *Ophthalmology*. 2013;120:1283–1291.
47. Coogan TA, Van Essen DC. Development of connections within and between areas V1 and V2 of macaque monkey. *J Comp Neurol*. 1996;372:327–342.
48. Butt OH, Benson NC, Datta R, Aguirre GK. The fine-scale functional connectivity of striate cortex in sighted and blind people. *J Neurosci*. 2013;33:16209–16219.
49. Aguirre GK, Komáromy AM, Cideciyan AV, et al. Canine and human visual cortex intact and responsive despite early retinal blindness from RPE65 mutation. *PLoS Med*. 2007;4:e230.
50. Bennett J, Ashtari M, Wellman J, et al. AAV2 gene therapy readministration in three adults with congenital blindness. *Sci Transl Med*. 2012;4:120ra15.
51. Ashtari M, Cyckowski LL, Monroe JF, et al. The human visual cortex responds to gene therapy-mediated recovery of retinal function. *J Clin Invest*. 2011;121:2160–2168.
52. Koenekoop RK, Sui R, Sallum J, et al. Oral 9-cis retinoid for childhood blindness due to Leber congenital amaurosis caused by RPE65 or LRAT mutations: an open-label phase 1b trial. *Lancet*. 2014;348:1513–1520.
53. Timberlake GT, Mainster MA, Peli E, Augliere RA, Essock EA, Arend LE. Reading with a macular scotoma. I. Retinal location of scotoma and fixation area. *Invest Ophthalmol Vis Sci*. 1986;27:1137–1147.
54. Baker CI, Peli E, Knouf N, Kanwisher NG. Reorganization of visual processing in macular degeneration. *J Neurosci*. 2005;25:614–618.
55. Dilks DD, Baker CI, Peli E, Kanwisher N. Reorganization of visual processing in macular degeneration is not specific to the "preferred retinal locus." *J Neurosci*. 2009;29:2768–2773.
56. Baker CI, Dilks DD, Peli E, Kanwisher N. Reorganization of visual processing in macular degeneration: replication and clues about the role of foveal loss. *Vision Res*. 2008;48:1910–1919.
57. Dilks DD, Julian JB, Peli E, Kanwisher N. Reorganization of visual processing in age-related macular degeneration depends on foveal loss. *Optom Vis Sci*. 2014;91:e199–206.

Investigative Ophthalmology & Visual Science